



# Synthesis and characterization of hybrid shell microcapsules for anti-corrosion Ni-Co coating

Hamed SADABADI<sup>1,2</sup>, Saeed Reza ALLAHKARAM<sup>1,\*</sup>, Omid GHADERI<sup>2</sup>, and Pradeep K. ROHATGI<sup>2</sup>

<sup>1</sup> School of Metallurgy and Materials Engineering, College of Engineering, University of Tehran, Tehran, 1417614411, Iran

<sup>2</sup> Department of Materials Science & Engineering, University of Wisconsin-Milwaukee, Milwaukee Wisconsin 53211, United States

\*Corresponding author e-mail: akaram@ut.ac.ir

## Received date:

12 September 2022

## Revised date

15 November 2022

## Accepted date:

16 November 2022

## Keywords:

Encapsulation;  
Microcapsule;  
Self-healing;  
Coatings;  
Nanostructure

## Abstract

This paper presents the results of the study of microcapsules synthesized using a novel hybrid shell of polyureaformaldehyde/SiO<sub>2</sub> (PUF/SiO<sub>2</sub>) and a core of linseed oil. The synthesis was accomplished by facial polymerization combined with sol-gel of TEOS, and urea-formaldehyde resin to form the hybrid shell under optimal process parameters. The microcapsules were embedded in a metal coating using the electrodeposition method. Microcapsules were characterized by scanning electron microscope (SEM, FE-SEM), energy-dispersive spectroscopy (EDS), particle size analyzer (PSA), thermogravimetric analysis (TGA), and differential scanning calorimetry (DSC). The experimental results indicated that the average size of capsules synthesized under the optimum processing parameters were in the range of 5 μm to 200 μm with a hybrid shell thickness of less than 1 μm. The internal surface of the shell contained more SiO<sub>2</sub> compared to the external PUF/SiO<sub>2</sub> layer, as indicated by EDS. While the internal surfaces were smooth, the outer surface of the microcapsules were composed of rough branched-like structures of urea-formaldehyde particles. It was shown by thermal analysis that initial decomposition starts at 225°C which proved excellent thermal stability. Electrodeposition was carried out with the current density of 25 mA·cm<sup>-2</sup> to embed the synthesized microcapsules into the Ni-Co alloy coating, which was investigated by SEM, and corrosion test (OCP, LP) to characterize the corrosion behavior of these potentially self-healing coatings.

## 1. Introduction

In 2016, the corrosion phenomenon was estimated to cost 2.5 trillion dollars globally (3.4% of global products). It is generally accepted that adequate corrosion mitigation techniques might save 15% to 35% of these costs [1-3]. Self-healing coatings can prevent corrosion of the substrate even after being damaged. These have been studied to enhance the lifetime of infrastructure equipment [4-8]. The two common strategies in creating autonomous self-healing coatings are capsule embedment and vascular systems [9,10]. Many techniques have been used in the past to synthesize nano/microcapsules [11-16], however, emulsion/in-situ polymerization and emulsion sol-gel, have become the most widely used methods for synthesizing capsules [17-19]. These methods have been used to synthesize organic shell nano/microcapsules, such as poly(urea-formaldehyde)[20], polystyrene [21], polyurethane [22], and polymethylmethacrylate due to the ease and feasibility of the procedure, as well as the controllability of shell thickness and size of the capsule [23]. Furthermore, the mechanical, physical, chemical, and biological properties and applications of polymeric microcapsules have also been widely studied [24-27].

Linseed oil (LO), the most common dry oil, exhibits promising healing and corrosion inhibition properties [27-30], therefore researchers have combined epoxy and commercial paint coatings with microcapsules

containing linseed oil to produce self-healing coatings [28-30]. Only a limited amount of research has been done on the incorporation of nano/microcapsules with a hybrid shell in metallic coatings to improve corrosion resistance and self-healing ability of metallic coatings [31-35] and this area is in particular interest.

In this paper, synthesis and characterization of nano/microcapsules with a hybrid (PUF/SiO<sub>2</sub>) shell have been reported. The mechanical and thermal properties of capsules may be enhanced by adding ceramic particles to the shell. This could extend storage period, increase durability against mechanical agitation during co-deposition, and increase resistance to higher temperature. Microcapsules were also incorporated into a nickel-cobalt alloy coating using the electrodeposition method, followed by the study of the structural, morphological, and corrosion properties of the coating.

## 2. Methodology

**Synthesis of microcapsules:** Tetraethylorthosilicate (TEOS), urea, and formaldehyde (37% aqueous solution) were used as shell precursors and linseed oil as a healing agent. Sodium dodecyl sulfate (SDS) was used as a surfactant, resorcinol, and hydrochloric acid as actuators for the polymerization process. Ethyl alcohol and xylene were used to

wash the residual oil on capsules. All the chemicals were purchased from Sigma-Aldrich and were used without further purification.

Microcapsules were produced by interfacial polymerization of TEOS over linseed oil droplets to generate initial shells. Then SiO<sub>2</sub> particles built the second shell over the initial shell followed by in-situ polymerization of urea and formaldehyde as the external shell. 2.5 mL of TEOS was dissolved in 30 mL of 100% ethanol in an ultrasonic bath at room temperature for 30 minutes to produce SiO<sub>2</sub> nanoparticles. Then, to facilitate TEOS hydrolysis in the ultrasonic bath, 5 mL of distilled water was added to the reaction media. After 30 min, 1 mL of HCl (catalyst) was slowly added to the reaction mixture. For 1 h, the mixture was stirred. This mixture was used as the source of SiO<sub>2</sub> particles for the next step.

A magnetic stirrer was used to mix TEOS with 5 mL linseed oil. Surfactant (2 wt% SDS) was added to 250 mL distilled water in a 500 mL beaker and the emulsion was then formed by adding core material and allowing it to stabilize for 30 min. To begin the reaction, the pH of the emulsion was adjusted to 3-4 by adding HCl and the temperature was raised to 70°C. SiO<sub>2</sub> nanoparticles, urea, resorcinol, and formaldehyde were added to the emulsion after 1 h of reaction time and agitated at 500 RPM. After 3, 6, and 18 h of reaction, samples were taken from the produced suspension of microcapsules, which were cooled to ambient temperature, filtered, rinsed with distilled water and diluted ethyl alcohol, then air-dried for 24 h. Table 1 shows the experimental parameters for the synthesis of microcapsules.

**Preparation of coating with microcapsules:** Ni-Co coatings incorporating microcapsules were electrodeposited from a bath with the composition of nickel sulfate (NiSO<sub>4</sub>·6H<sub>2</sub>O), 250 g·L<sup>-1</sup>; cobalt sulfate (CoSO<sub>4</sub>·7H<sub>2</sub>O), 25 g·L<sup>-1</sup>; boric acid (H<sub>3</sub>BO<sub>3</sub>), 30 g·L<sup>-1</sup> (buffer); saccharin (C<sub>7</sub>H<sub>5</sub>NO<sub>3</sub>S), 0.5 g·L<sup>-1</sup>, and microcapsules at 0 and 30 g·L<sup>-1</sup>. All chemicals were purchased from Sigma-Aldrich and were used without further purification. The electrolyte pH was maintained at pH 5.0 and the temperature set at 40°C to 45°C. The electrodeposition was carried out on a 21 mm × 21 mm mild steel plate, with a direct current (DC) density of 25 mA·cm<sup>-2</sup> for 30 min. The mild steel substrate

(up to 0.25 wt% carbon) was initially polished, degreased in acetone for 5 min, and surface activated in 3.6% HCl for 30 s. The substrate was subsequently rinsed thoroughly with distilled water and placed in the deposition bath immediately. Magnetic stirring was applied at 200 RPM throughout the entire process to maintain the uniform distribution of the capsules and ions during electrodeposition.

The size, morphology, and composition of the microcapsules, as well as the shell thickness, were studied with the scanning electron microscope (SEM, JEOL 6460LV), FE-SEM (Hitachi S-4800), and particle size analyzer (MASTERSIZE3000). Thermogravimetry (TGA, TA SDT650) and differential scanning calorimetry (DSC, TA SDT650) were used in an argon atmosphere to measure the thermal stability of the microcapsules. Corrosion characterization was done using the BioLogic SP-200.

### 3. Results and discussion

FE-SEM micrographs revealed that the microcapsules were spherical in shape (Figure 2), and the rough surface and branch-like structures are formed of UF and perform as a hook to improve bonding with the matrix material and improve surface adhesion. SEM micrographs revealed that the percentage of broken capsules increased with an increase in reaction times, possibly due to magnetic stirring and subsequent capsule collision.

The shell thickness was less than 1 μm for samples with an 18 h reaction time (Figure 3(a)), allowing for a higher carrying load of healing agent and enhanced healing efficiency. Furthermore, the microcapsules' smooth and dense inner surface can prevent the healing agent from leaking out during storage. The microcapsules were immersed in 100% acetone for 3 h and SEM micrographs were taken to assess the durability of the hybrid shell to solvent exposure (see Figure 3(b)). The surface of the microcapsules did not change significantly. SEM micrographs showed that the capsules could withstand exposure to a severe solvent.

**Table 1.** Sample numbers and experimental parameters for microcapsules.

Sample No.	Core/shell ratio (g)	TEOS/polymer ratio (g)	Stirring (RPM)	Reaction time (h)	pH
SG-01-01	5:6	1:1	500	18	3-4
SG-01-02	5:6	1:1	500	6	3-4
SG-01-03	5:6	1:1	500	3	3-4

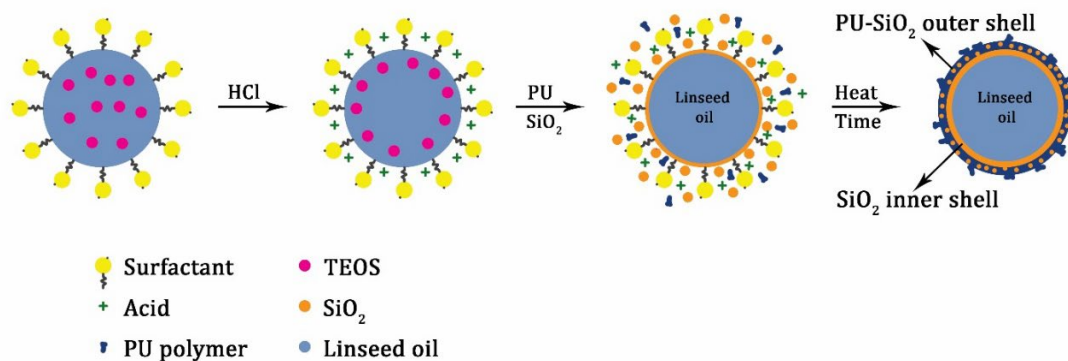


**Figure 1.** Schematic representation of encapsulation process for the hybrid shell with linseed oil as core material.

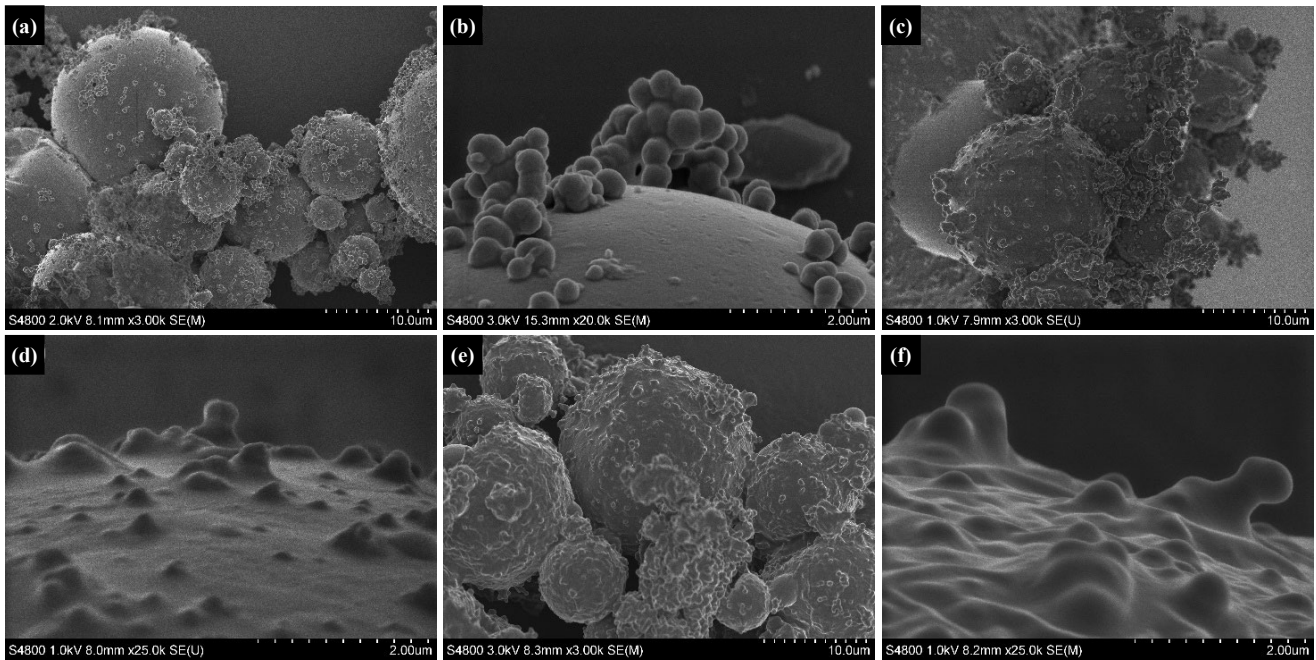


**Figure 2.** FE-SEM micrographs of samples number SG-01-01 after 18 h (a, b), SG-01-02 after 6 h (c, d), and SG-01-03 after 3 h (e, f) reaction time.

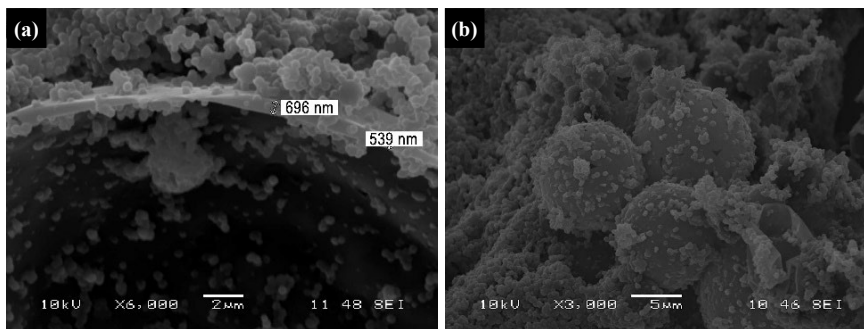


**Figure 3.** SEM micrographs of (a) microcapsules shell SG-01-01, (b) after 3 h soaking in absolute acetone of sample SG-01-01.

EDS analysis of the capsules' external and internal surfaces (Figure 4) validated the proposed capsule formation mechanism. A thin silica shell formed around the core materials at first, which was then covered by PUF and SiO<sub>2</sub> particles. The presence of silica in the outer layer reduced as the reaction time increased. Moreover, surfaces of capsules were smoother in samples made with shorter reaction time, indicating that the surface spots were caused by UF nanoparticle precipitation on the initial silica shell.

The size distribution of microcapsules synthesized with different reaction time durations is shown in Table 2. It can be interpreted from Table 2 that nanoparticles of UF and SiO<sub>2</sub> were synthesized in the emulsion, and then these particles connected to the initial silica shell, leading their size to increase.

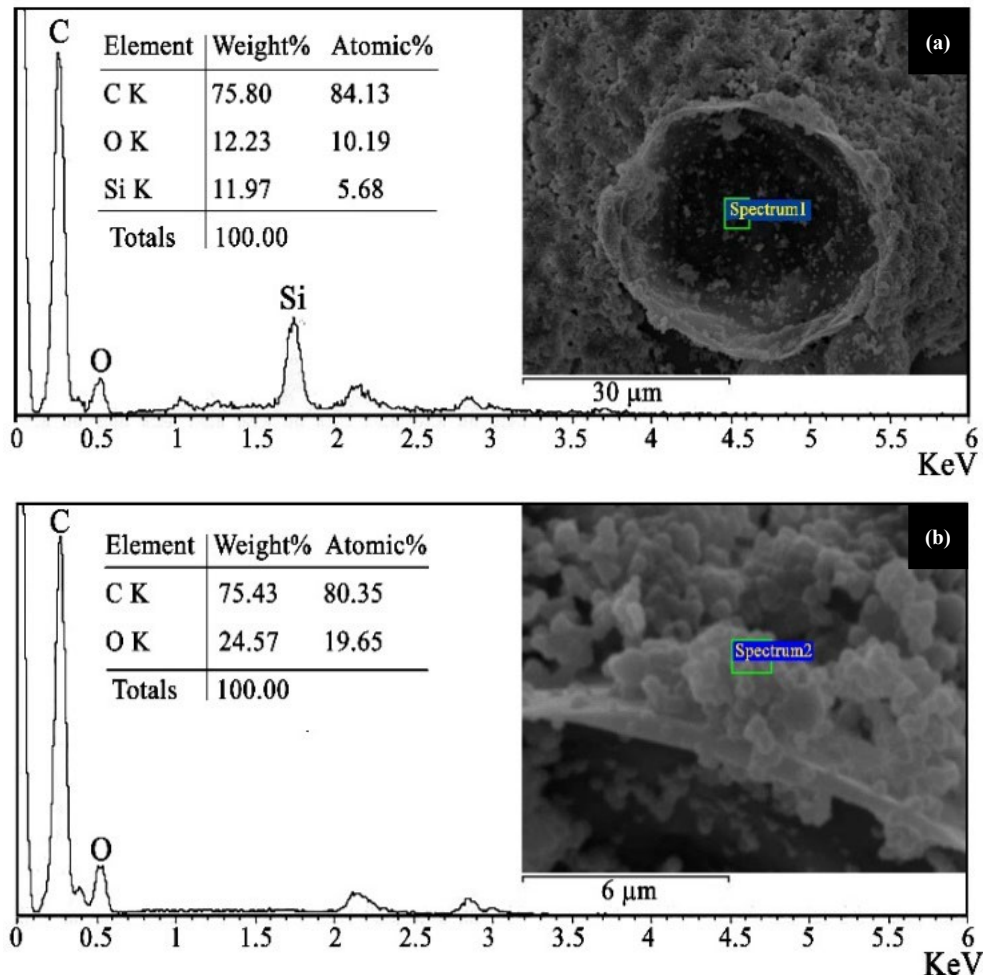
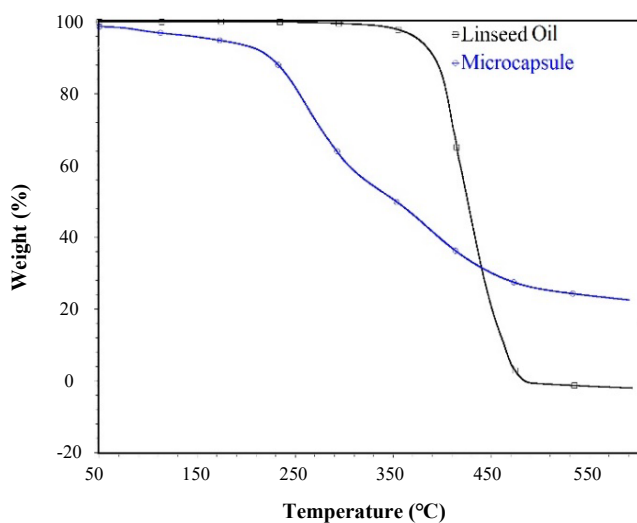
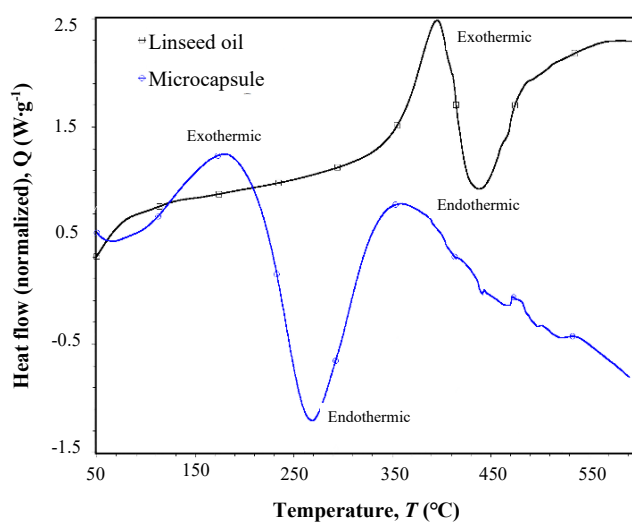
The thermal stability of capsules is important for their use in self-healing coatings. In this study, the thermal stability of the capsules was investigated using Thermogravimetric Analyses (TGA) (Figure 5) and Differential Scanning Calorimetry (DSC) (Figure 6). Because oxygen absorption causes a mass increase in linseed oil at temperatures between 50°C and 150°C in an oxidant environment, studies were

conducted in an argon atmosphere. TGA curves of capsules and linseed oil are shown in Figure 5. The first change in weight, which took place below 100°C, involved the evaporation of moisture and free formaldehyde. The second change in weight involved the decomposition of the shell, and the third involved the combustion of by-products from the previous steps as well as residual silica. Changes in the slope were observed around 350°C, where linseed decomposition of oil began, which was attributable to shell fracture and subsequent release of the core material.

The DSC analysis in Figure 6 shows that evaporation of moisture and free formaldehyde caused the first endothermic peak at 90°C, while the decomposition of shell materials caused the second one at 270°C. It's possible that the first exothermic peak, which occurred between 150°C and 180°C, was caused by residual core materials. The peak at 350°C was caused by the polymerization reaction of the core material, which is initiated by urea derivatives, as well as the gaseous products generated by the decomposition of UF in the outer shell material and the self-condensation of the core material [36].

**Table 2.** Particle size analysis of samples with different reaction times.

Sample No.	SG 01-01	SG 01-02	SG 01-03
Dv (10) $\mu\text{m}$	7.04	0.377	0.251
Dv (50) $\mu\text{m}$	56.2	14.6	3.34
Dv (90) $\mu\text{m}$	144	74.4	74.4

**Figure 4.** EDS analysis of sample number SG-01-01 microcapsules' (a) inner, (b) outer shell.**Figure 5.** TGA analysis of SG-01-01 microcapsules and linseed oil.**Figure 6.** DSC analysis of SG-01-01 microcapsules and linseed oil.

The SEM surface morphology and cross-sections image of Ni-Co/microcapsule co-deposited coating and pristine Ni-Co coating (Figure 7) showed that a microcapsules had co-deposited with a dense coating on the substrate with a thickness of about  $\sim 30 \mu\text{m}$ . The morphology changes observed are result of capsule co-deposition (Figure 7(a) and 7(c)).

The corrosion behavior of nanocrystalline coatings was evaluated by open circuit potential (OCP) and linear polarization (LP) methods after 8 h of conditioning at room temperature, as described below. The OCP diagram in Figure 8 showed significant improvement when capsules were incorporated into the coating. Also, it was indicated that there was a slight increase of OCP during the time, which may be due to the rupture of the facial capsules and release of oil during the characterization. The auto-oxidation process could begin with double bonds which absorb dissolved oxygen in water, followed by

a polymerization reaction involving cross-linking, and eventually, the formation of a solid and adherent film on the surface that acts as a protective layer on the substrate.

Figure 9 shows the linear polarization curves of the substrate, Ni-Co alloy coating with capsules, and coating without microcapsules recorded during corrosion tests in the 3.5% NaCl corrosive medium at room temperature. The electrochemical data extracted from linear polarization curves were summarized in Table 3, which showed that the corrosion current gradually decreased from  $3.13 \mu\text{A}\cdot\text{cm}^{-2}$  for the substrate to  $0.19 \mu\text{A}\cdot\text{cm}^{-2}$ , and  $0.081 \mu\text{A}\cdot\text{cm}^{-2}$  for the Ni-Co coating and coating with  $30 \text{ g}\cdot\text{L}^{-1}$  microcapsules respectively. Dramatic increases in the corrosion resistance of deposited alloys may be correlated to several important factors such as chemical composition, phase composition, texture or preferred orientation, grain size, residual stresses, defects (porosity), surface morphology, and roughness.

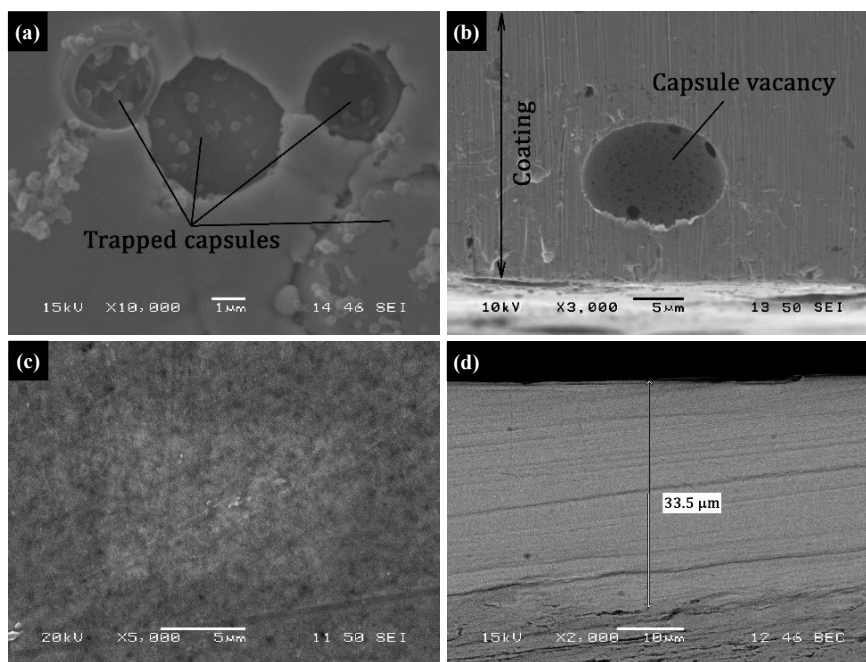


**Figure 7.** SEM images of (a) surface morphology of Ni-Co coating with capsule SG-01-01, (b) cross-section of Ni-Co/microcapsule, (c) surface morphology of pristine Ni-Co coating, (d) cross-section of pristine Ni-Co electrodeposited coating.

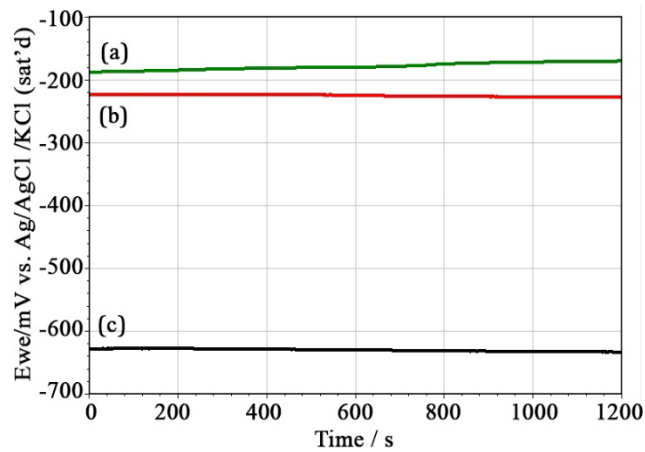


**Figure 8.** OCP diagram of (a) Ni-Co coating with  $30 \text{ g}\cdot\text{L}^{-1}$  microcapsules of SG-01-01, (b) pristine Ni-Co coating deposited at  $25 \text{ mA}\cdot\text{cm}^{-2}$  direct current, and (c) substrate without coating.

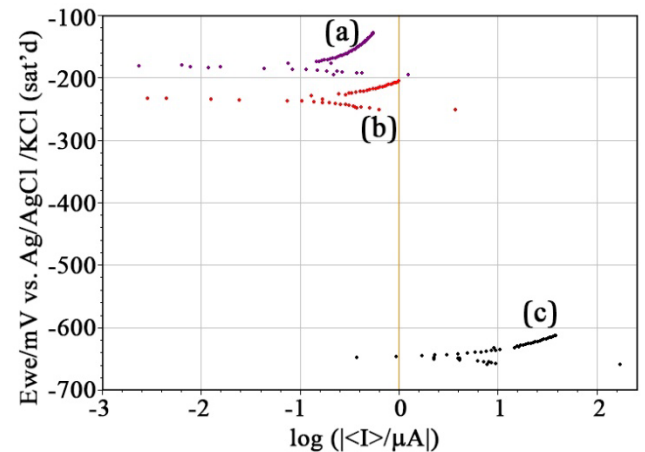


**Figure 9.** LP diagram of (a) Ni-Co coating with  $30 \text{ g}\cdot\text{L}^{-1}$  microcapsules of SG-01-01, (b) pristine Ni-Co coating deposited at  $25 \text{ mA}\cdot\text{cm}^{-2}$  direct current, and (c) substrate without coating.

**Table 3.** Electrochemical data of the Ni-Co alloy coatings extracted from linear polarization curves.

Sample	Substrate	Ni-Co	Ni-Co/MC
R <sub>p</sub> (Ω)	1372	30690	60300
E <sub>corr</sub> (mV vs. Ref)	-649.50	-235.27	-185.67
I <sub>corr</sub> (μA·cm <sup>-2</sup> )	3.130	0.190	0.081
Corrosion rate (mpy)	1.74273	0.09335	0.03979
β <sub>a</sub>	30.5	27.6	39.8
β <sub>c</sub>	15.7	26.1	10.2

#### 4. Conclusions

In the present study, microcapsules with hybrid shells of PUF and silica were successfully produced using a combination of interfacial/sol-gel polymerization where linseed oil was encapsulated within the microcapsules. In this process, all parameters were kept at the optimum values as determined by previous research on single-composition shells, with the exception of elapsed reaction time which was used to investigate the effects of reaction time on the morphology of microcapsules. The thickness of the microcapsule shell was less than 1 μm in most cases.

The results showed that microcapsules with a hybrid shell and an average size of less than 200 μm could be successfully synthesized. EDS characterization of the external and internal surfaces of the capsules confirmed the proposed capsule formation mechanism (Figure 1). The roughness of surface texture made of PUF also improved with increasing reaction time. This study also confirmed the thermal and structural stability of the produced capsules, thus enhancing the feasibility of hybrid capsule utilization.

The results showed that the corrosion resistance of the capsule-embedded coating was significantly improved compared to the pristine coating.

Hybrid capsules can now be used in a wider range of applications, including self-healing coatings and corrosion-resistant composites of both metallic and non-metallic compositions.

#### Acknowledgements

The authors thank Dr. Steven Hardcastle from Advanced Analysis Facility (AAF) and Dr. Heather Owen at UWM for their helpful advices on the characterization results of the materials employed in this study.

#### References

- [1] B. Hou, X. Li, X. Ma, C. Du, D. Zhang, M. Zheng, W. Xu, D. Lu, F. Ma, "The cost of corrosion in China," *npj Materials Degradation*, vol. 1, no. 1, p. 4, 2017.
- [2] F. Zhang, P. Ju, M. Pan, D. Zhang, Y. Huang, G. Li, X. Li, "Self-healing mechanisms in smart protective coatings: A review," *Corrosion Science*, vol. 144, pp. 74-88, 2018.
- [3] H. Sadabadi, O. Ghaderi, A. Kordijazi, and P. K. Rohatgi, "Graphene derivatives reinforced metal matrix nanocomposite coatings: A review," *Journal of Metals, Materials and Minerals*, vol. 32, no. 3, pp. 1-14, 2022.
- [4] A. Stankiewicz, I. Szczygiel, and B. Szczygiel, "Self-healing coatings in anti-corrosion applications," *Journal of Materials Science*, vol. 48, no. 23, pp. 8041-8051, 2013.
- [5] A. Stankiewicz, "Self-healing nanocoatings for protection against steel corrosion," in *Nanotechnology in Eco-efficient Construction*, Elsevier, 2019, pp. 303-335.
- [6] M. S. Koochaki, S. N. Khorasani, R. E. Neisiany, A. Ashrafi, S. P. Trasatti, and M. Magni, "A highly responsive healing agent for the autonomous repair of anti-corrosion coatings on wet surfaces. In operando assessment of the self-healing process," *Journal of Materials Science*, vol. 56, no. 2, pp. 1794-1813, 2021.
- [7] E. Adibzadeh, S. M. Mirabedini, M. Behzadnasab, and R. R. Farnood, "A novel two-component self-healing coating comprising vinyl ester resin-filled microcapsules with prolonged anticorrosion performance," *Progress in Organic Coatings*, vol. 154, p. 106220, May 2021.
- [8] W. Chen, T. Yang, L. Dong, A. Elmasry, J. Song, N. Deng, A. Elmarakbi, T. Liu, H. B. Lv, Y. Q. Fu, "Advances in graphene reinforced metal matrix nanocomposites: Mechanisms, processing, modelling, properties and applications," *Nanotechnology and Precision Engineering*, vol. 3, no. 4, pp. 189-210, 2021.
- [9] M. Srinivas, B. Yelamasetti, T. Vishnu Vardhan, and R. Mohammed, "A critical review on self-healing composites," *Materials Today: Proceedings*, vol. 46, pp. 890-895, 2021.
- [10] V. Kilicli, X. Yan, N. Salowitz, and P. K. Rohatgi, "Recent advancements in self-healing metallic materials and self-healing metal matrix composites," *JOM*, vol. 70, no. 6, pp. 846-854, Jun. 2018.
- [11] R. Ciriminna, M. Sciortino, G. Alonzo, A. De Schrijver, and M. Pagliaro, "From molecules to systems: Sol-gel microencapsulation in silica-based materials," *Chemical Reviews*, vol. 111, no. 2, pp. 765-789, 2011.
- [12] A. M. Bakry, S. Abbas, B. Ali, H. Majeed, M. Abouelwafa, A. Mousa, L. Liang, "Microencapsulation of oils: A comprehensive review of benefits, techniques, and applications," *Comprehensive Reviews in Food Science and Food Safety*, vol. 15, no. 1, pp. 143-182, 2016.
- [13] S. K. Ghosh, "Functional coatings and microencapsulation: A general perspective," in *Functional Coatings*, Weinheim, FRG: Wiley-VCH Verlag GmbH & Co. KGaA, 2006, pp. 1-28.
- [14] S. M. Jafari, "An overview of nanoencapsulation techniques and their classification," in *Nanoencapsulation Technologies for the Food and Nutraceutical Industries*, Elsevier, 2017, pp. 1-34.
- [15] S. H. Soh and L. Y. Lee, "Microencapsulation and nanoencapsulation using supercritical fluid (SCF) techniques," *Pharmaceutics*, vol. 11, no. 1, p. 21, 2019.

- [16] H. Sadabadi, S. R. Allahkaram, A. Kordijazi, and P. K. Rohatgi, "Self-healing coatings loaded by nano/microcapsules: A review," *Protection of Metals and Physical Chemistry of Surfaces*, vol. 58, no. 2, pp. 287-307, 2022.
- [17] J. D. Rule, N. R. Sottos, and S. R. White, "Effect of microcapsule size on the performance of self-healing polymers," *Polymer*, vol. 48, no. 12, pp. 3520-3529, 2007.
- [18] M. L. Zheludkevich, J. Tedim, and M. G. S. Ferreira, "Smart coatings for active corrosion protection based on multi-functional micro and nanocontainers," *Electrochimica Acta*, vol. 82, pp. 314-323, 2012.
- [19] O. Nguon, F. Lagugné-Labarthe, F. A. Brandys, J. Li, and E. R. Gillies, "Microencapsulation by in situ Polymerization of Amino Resins," *Polymer Reviews*, vol. 58, no. 2, pp. 326-375, 2018.
- [20] S. Lang, and Q. Zhou, "Synthesis and characterization of poly(urea-formaldehyde) microcapsules containing linseed oil for self-healing coating development," *Progress in Organic Coatings*, vol. 105, pp. 99-110, 2017.
- [21] A. Sari, C. Alkan, D. K. Döğüçü, and C. Kizil, "Micro/nano encapsulated n-tetracosane and n-octadecane eutectic mixture with polystyrene shell for low-temperature latent heat thermal energy storage applications," *Solar Energy*, vol. 115, pp. 195-203, 2015.
- [22] P. Kardar, "Preparation of polyurethane microcapsules with different polyols component for encapsulation of isophorone diisocyanate healing agent," *Progress in Organic Coatings*, vol. 89, pp. 271-276, 2015.
- [23] F. Ahangaran, M. Hayaty, and A. H. Navarchian, "Morphological study of polymethyl methacrylate microcapsules filled with self-healing agents," *Applied Surface Science*, vol. 399, pp. 721-731, 2017.
- [24] S. Deng, M. R. Giglio Bianco, R. Censi, and P. Di Martino, "Polymeric nanocapsules as nanotechnological alternative for drug delivery system: Current status, challenges and opportunities," *Nanomaterials*, vol. 10, no. 5, p. 847, 2020.
- [25] T. Bollhorst, K. Rezwan, and M. Maas, "Colloidal capsules: Nano- and microcapsules with colloidal particle shells," *Chemical Society Reviews*, vol. 46, no. 8, pp. 2091-2126, 2017.
- [26] N. Shahabudin, R. Yahya, and S. N. Gan, "Microcapsules of poly(urea-formaldehyde) (PUF) containing alkyd from palm oil," *Materials Today: Proceedings*, vol. 3, no. Icfmd 2015, pp. S88-S95, 2016.
- [27] S. R. Whites, E. N. Brown, M. R. Kessler, and N. R. Sottos, "In situ poly(urea-formaldehyde) microencapsulation of dicyclopentadiene," *Journal of Microencapsulation*, vol. 20, no. 6, pp. 719-730, 2003.
- [28] C. Suryanarayana, K. C. Rao, and D. Kumar, "Preparation and characterization of microcapsules containing linseed oil and its use in self-healing coatings," *Progress in Organic Coatings*, vol. 63, no. 1, pp. 72-78, 2008.
- [29] T. Szabó, J. Telegdi, and L. Nyikos, "Linseed oil-filled microcapsules containing drier and corrosion inhibitor - Their effects on self-healing capability of paints," *Progress in Organic Coatings*, vol. 84, pp. 136-142, 2015.
- [30] G. Kurt Çömlekçi, and S. Ulutan, "Acquired self-healing ability of an epoxy coating through microcapsules having linseed oil and its alkyd," *Progress in Organic Coatings*, vol. 129, no. July 2018, pp. 292-299, 2019.
- [31] Z. Liqun, Z. Wei, L. Feng, and Y. He, "Electrodeposition of composite copper/liquid-containing microcapsule coatings," *Journal of Materials Science*, vol. 39, no. 2, pp. 495-499, 2004.
- [32] X. Xu, H. Liu, W. Li, and L. Zhu, "A novel corrosion self-protective copper/liquid microcapsule composite coating," *Materials Letters*, vol. 65, no. 4, pp. 698-701, 2011.
- [33] X. Q. Xu, L. Q. Zhu, W. P. Li, and H. C. Liu, "Microstructure and deposition mechanism of electrodeposited Cu/liquid microcapsule composite," *Transactions of Nonferrous Metals Society of China (English Edition)*, vol. 21, no. 10, pp. 2210-2215, 2011.
- [34] O. S. Kholkin, A. P. Kurbatov, G. W. Beall, T. Djenizian, A. K. Galeyeva, M. S. Lepikhin, S. T. Kokhmetova, "Effect of current density on electrodeposition of nickel-organic microcapsules composite coatings," *Eurasian Chemico-Technological Journal*, vol. 16, no. 4, pp. 277-286, 2014.
- [35] S. Alexandridou, C. Kiparissides, J. Fransaeer, and J. P. Celis, "On the synthesis of oil-containing microcapsules and their electrolytic codeposition," *Surface and Coatings Technology*, vol. 71, no. 3, pp. 267-276, 1995.
- [36] T. E. Sadrabadi, S. R. Allahkaram, T. Staab, and N. Towhidi, "Preparation and characterization of durable micro/nano-capsules for use in self-healing anticorrosive coatings," *Polymer Science - Series B*, vol. 59, no. 3, pp. 281-291, 2017.